Fracture Mechanics of Concrete Structures, de Borst et al (eds) © 2001 Swets & Zeitlinger, Lisse, ISBN 90 2651 825 0

An elastoplastic-damage model for quasi brittle materials in the framework of the strong discontinuity approach

Jörn Mosler & Günther Meschke
Institute for Structural Mechanics, Ruhr-University Bochum, Germany

ABSTRACT: In the paper, an anisotropic elastoplastic-damage model is formulated in the context of the strong discontinuity approach (SDA) (Simo, Oliver, and Armero 1993) for Finite Element (FE) analysis of mode-I fracture in quasi brittle materials. The constitutive relations of the elastoplastic-damage material degenerate to traction-displacement relations at the line of discontinuity. As a consequence, no special internal length parameter needs to be introduced. The equations are integrated exactly without any numerical parameter. The parameter defining the amplitude of the displacement jump within the finite element is condensed out at the material level without employing the standard static condensation technique. This approach results in a form of the linearized constitutive equations formally identical to continuum models. Therefore the standard return mapping algorithm is used to solve the nonlinear equations. Algorithmic issues and details of the implementation are discussed with emphasis on unloading and reloading conditions. The applicability of the SDA finite element model as well as its numerical performance is investigated by means of a representative example.

1 INTRODUCTION

Numerical analyses of structures made of brittle materials loaded up and beyond a critical level, at which cracks start to open, require special considerations to obtain objective results with regards to mesh refinement. Nonlocal models that make use of an internal length parameter related to the specific material are one possible choice. This approach, however, requires a sufficiently fine resolution of the crack zone to guarantee mesh objectivity resulting in high computer cost for large scale computations even if adaptive techniques are used. As an alternative method, the fracture zone can be represented as a line of discontinuous displacements within the respective finite elements. This method allows to use relatively large elements compared to the size of the crack width.

The idea to enhance standard finite element models by additional modes to capture displacement jumps was suggested already in the early work by (Johnson and Scott 1981). A more detailed insight into the effect of strong discontinuities in classical continuum models was given in (Simo, Oliver, and Armero 1993). In an effort to simulate the brittle response of concrete structures the concept was also used in the context of damage theory (Armero 1997).

In the present paper, the strong discontinuity approach is extended to a rotating localization surface approach to reduce locking effects. This aspect has also recently been addressed by (Jirásek 2001). In contrast to previous formulations of the SDA, an anisotropic elastoplastic damage model suggested by (Meschke, Lackner, and Mang 1998) is formulated within the framework of the SDA. The benefit of this model is a more realistic representation of the un- and reloading behavior of cracked brittle materials. This SDA-based model is formulated in an identical manner as classical continuum-based models. Hence, the usual static condensation of the parameter defining the displacement jump is circumvented. The analogy of its algorithmic formulation with formulations for standard plasticity models is demonstrated.

2 KINEMATICS: DISCONTINUOUS DISPLACEMENT FIELDS

A domain Ω of a body $\mathcal{B}$ is considered to be separated into two portions Ω^- and Ω^+ by means of a localization surface $\partial_S\Omega$ (Fig. 1). This surface is defined by its normal n. Based on the assumption of a jump in the displacement field across this surface, an additive decomposition of the displacement field

$$u(x) = \bar{u}(x) + \hat{u}(x), \qquad \forall x \in \Omega, \tag{1}$$

with

$$\hat{u}(x) = [\![u]\!]\, M_S(x). \tag{2}$$

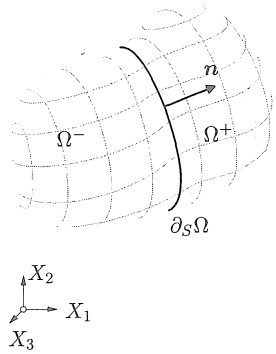

Figure 1: Body $\mathcal{B}$ separated by a localization surface $\partial_S\Omega$ into two parts Ω^- and Ω^+

into a regular part $\bar{u}(x)$ and a jump term $\hat{u}(x)$ is motivated (Simo, Oliver, and Armero 1993) (Fig. 2).

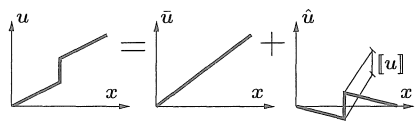

Figure 2: Additive decomposition of the displacement field into a regular part $\bar{u}$ and a part $\hat{u}$ which contains a jump

The function $M_S(x)$ can also be decomposed into a HEAVISIDE function $H_S(x)$ and a smooth function $\varphi(x)$ (Simo, Oliver, and Armero 1993)

$$M_S(x) = H_S(x) - \varphi(x), \qquad \forall x \in \Omega. \tag{3}$$

The function $\varphi(x)$ allows to prescribe the boundary conditions in terms of $\bar{u}$. At the localization surface

$$[\![M_S(x)]\!] = 1, \qquad \forall x \in \partial_S\Omega \tag{4}$$

has to be fulfilled. From computing the gradient of Eq. (1), using Eqs. (2) and (3), the linearized strain tensor is obtained as

$$\begin{aligned} \varepsilon(u) = \nabla^{\text{sym}} u \;&= \nabla^{\text{sym}} \bar{u} - \underbrace{([\![u]\!] \otimes \nabla\varphi)^{\text{sym}}}_{\tilde{\varepsilon}} \\ &+ \underbrace{([\![u]\!] \otimes n)^{\text{sym}}}_{\varepsilon_\delta} \delta_S. \end{aligned} \tag{5}$$

The modified strain tensor (5) contains, in addition to the gradient of the smooth part of the displacement field, two additional parts, $\tilde{\varepsilon} \in \Omega$ and $\varepsilon_\delta \in \partial_S\Omega$. To simplify the following derivations, the decomposition of the discontinuous displacement field

$$[\![u]\!] = \zeta\, m \tag{6}$$

into a vector m, defining the direction of the jump, and the amplitude of the jump ζ is introduced. The vectors n and m are computed from a bifurcation analysis, characterized by the localization condition

$$Q^{\text{perf}} \cdot m = 0, \tag{7}$$

with the acoustic tensor Q^{perf} defined as

$$Q^{\text{perf}} = n \cdot \mathbb{C}_T^{\text{perf}} \cdot n. \tag{8}$$

In contrast to classical bifurcation condition Q^{perf} is based on the perfect plastic tangent (Simo, Oliver, and Armero 1993).

3 MATERIAL MODELS CONSIDERING JUMPS IN THE DISPLACEMENT FIELD

In this section, the incorporation of two different classes of material models within the framework of the Strong Discontinuity Approach is addressed. In Subsection 3.1, the formulation of classical plasticity models is discussed to give a concise summary of the standard approach. Subsection 3.2 contains the respective SDA-formulation for an anisotropic combined plasticity-damage model. Comparing both subsections reveals the analogy between both formulations.

3.1 Plasticity theory

In this subsection, the concept of strong discontinuities is incorporated within the governing equations of classical nonassociated plasticity theory. The flow-rule and the plastic multiplier are re-formulated in a general context within the framework of the SDA. Then, the principal stress model is taken as a particular example.

Without referring to any particular model of plasticity for now, the space of admissible stresses

$$\mathbb{E}_\sigma := \{(\sigma, q) \in \mathbb{S} \times \mathrm{R} \,|\phi(\sigma, q) \leq 0\} \tag{9}$$

is defined by means of a yield (failure) function $\phi(\sigma, q)$, which depends on the stress tensor and a stress-like hardening/softening parameter q. The model is completed with the definition of the stress rate and the evolution of the plastic strains

$$\begin{aligned} \dot{\sigma} &= \mathbb{C} : (\dot{\varepsilon} - \dot{\varepsilon}^{\text{p}}), \\ \dot{\varepsilon}^{\text{p}} &= \lambda \frac{\partial g(\sigma, q)}{\partial \sigma}, \qquad \lambda \geq 0, \quad \lambda\, \phi = 0, \\ \dot{\alpha} &= \lambda \frac{\partial g(\sigma, q)}{\partial q}, \end{aligned} \tag{10}$$

where $g(\sigma, q)$ is a potential function. From the regular distribution of the stress tensor follows, that the plastic multiplier λ

$$\lambda = \bar{\lambda} + \lambda_\delta \delta_S. \tag{11}$$

must exhibit a singular part (Simo, Oliver, and Armero 1993). Assuming $\bar{\lambda} = 0$, additional plastic deformations are restricted to the surface of discontinuity $\partial_S\Omega$, while in the remaining part of the considered domain

$$\dot{\boldsymbol{\varepsilon}}^{\mathrm{p}} = \mathbf{0}, \quad \forall\, \boldsymbol{x} \in \Omega^-, \Omega^+. \tag{12}$$

From Eq. (12) and from the traction continuity requirement follows, that the plastic strains $\boldsymbol{\varepsilon}^{\mathrm{p}}$ are related to the assumed singular strains

$$([\![\boldsymbol{u}]\!] \otimes \boldsymbol{n})^{\mathrm{sym}} = \lambda_\delta \frac{\partial g(\boldsymbol{\sigma}, \boldsymbol{q})}{\partial \boldsymbol{\sigma}}. \tag{13}$$

Using the consistency condition $\dot{\phi} = 0$, the singular plastic multiplier λ_δ can be computed by means of the amplitude of the displacement jump ζ as

$$\lambda_\delta = \dot{\zeta} \frac{\partial_{\boldsymbol{\sigma}} \phi : \mathbb{C} : (\boldsymbol{m} \otimes \boldsymbol{n})^{\mathrm{sym}}}{\partial_{\boldsymbol{\sigma}} \phi : \mathbb{C} : \partial_{\boldsymbol{\sigma}} g}. \tag{14}$$

In what follows, the simple case of positively homogeneous yield functions of degree one, e.g.

$$\phi(\boldsymbol{\sigma}, \zeta) = (\boldsymbol{m} \otimes \boldsymbol{n}) : \boldsymbol{\sigma} - q(\zeta), \tag{15}$$

together with an associative flow model will be used. For the special case $\boldsymbol{m} = \boldsymbol{n}$, the RANKINE failure criterion, suitable for the representation of mode-I failure in brittle materials, is recovered. In this case, $\boldsymbol{n}$ coincides with the direction of the maximal principal the stress. The stress component $(\boldsymbol{n} \otimes \boldsymbol{n}) : \boldsymbol{\sigma} \leq \sigma_{\max}$ normal to the fracture surface is controlled by the failure criterion. In the numerical analysis contained in Section 5, this type of failure criterion will be employed within the framework of the elastoplastic-damage model described in the next subsection.

3.2 Elastoplastic damage model

In this subsection, a phenomenological anisotropic elastoplastic damage model proposed by (Meschke, Lackner, and Mang 1998) is re-formulated within the concept of strong discontinuities. Here, only mode-I fracture of brittle solids is taken into consideration. A similar formulation of continuum damage has been employed by (Armero 1997), using a fixed crack approach in conjunction with the SDA. Here, a different approach is taken for the incorporation of the combined plasticity-damage model within the context of the SDA. The difference is particularly manifested in the modeling of un- and reloading cycles. The proposed formulation allows for a consistent description of un- and reloading branches also for rotating crack formulations in full analogy to elastoplastic models.

The constitutive model is based on the following form of the free energy

$$\begin{aligned} \Psi(\boldsymbol{\varepsilon}, \boldsymbol{\varepsilon}^{\mathrm{p}}, \boldsymbol{C}, \alpha) \;&= \frac{1}{2}(\boldsymbol{\varepsilon} - \boldsymbol{\varepsilon}^{\mathrm{p}}) : \mathbb{C} : (\boldsymbol{\varepsilon} - \boldsymbol{\varepsilon}^{\mathrm{p}}) \\ &\quad + S(\alpha), \end{aligned} \tag{16}$$

where α is an internal variable.

The rate of the enhanced strains in Ω^+ and Ω^- is given as

$$\begin{aligned} \dot{\tilde{\boldsymbol{\varepsilon}}} = ([\![\dot{\boldsymbol{u}}]\!] \otimes \boldsymbol{n})^{\mathrm{sym}} &= (\boldsymbol{m} \otimes \boldsymbol{n})^{\mathrm{sym}} \quad \dot{\zeta} \\ &= \boldsymbol{G} \quad \dot{\zeta}. \end{aligned} \tag{17}$$

For the tensor of enhanced strains, the following split

$$\dot{\tilde{\boldsymbol{\varepsilon}}} = \underbrace{\dot{\tilde{\boldsymbol{\varepsilon}}}^{\mathrm{d}}}_{\mathbb{D} : \boldsymbol{\sigma}} + \dot{\tilde{\boldsymbol{\varepsilon}}}^{\mathrm{p}}. \tag{18}$$

is assumed. In Eq. (18), $\dot{\tilde{\boldsymbol{\varepsilon}}}^{\mathrm{d}}$ represents rates of enhanced strains related to the stiffness degradation and $\dot{\tilde{\boldsymbol{\varepsilon}}}^{\mathrm{p}}$ are rates related to inelastic strains. The rates of both enhanced strains $\dot{\tilde{\boldsymbol{\varepsilon}}}^{\mathrm{d}}$ and $\dot{\tilde{\boldsymbol{\varepsilon}}}^{\mathrm{p}}$ are associated with the opening of cracks characterized by the crack normal $\boldsymbol{n}$. In case of mode-I failure in brittle materials, permanent deformations result from imperfect crack closure due to the roughness of the crack faces. Introducing a scalar parameter β, a simple decomposition of the pseudo plastic and the damage strains yields

$$\begin{aligned} \dot{\tilde{\boldsymbol{\varepsilon}}}^{\mathrm{d}} &= \dot{\mathbb{D}} : \boldsymbol{\sigma} = \beta \quad \boldsymbol{G}\, \dot{\zeta}, \\ \dot{\tilde{\boldsymbol{\varepsilon}}}^{\mathrm{p}} &= (1 - \beta) \quad \boldsymbol{G}\, \dot{\zeta}, \end{aligned} \qquad \forall \beta \in [0, 1]. \tag{19}$$

It should be noted, that this type of a linear decomposition of the enhanced strains into portions related to the degradation of the stiffness tensor and to inelastic deformations, respectively, is only a crude approximation of the more complex coupling mechanisms associated with the opening and closure of cracks.

The evolution of the compliance tensor remains to be defined. Double contraction of $\dot{\tilde{\boldsymbol{\varepsilon}}}^{\mathrm{d}}$ with the stress tensor $\boldsymbol{\sigma}$ and multiplication by $(\partial_{\boldsymbol{\sigma}} \phi : \boldsymbol{\sigma})/(\partial_{\boldsymbol{\sigma}} \phi : \boldsymbol{\sigma})$ yields after some algebraic transformations

$$\begin{aligned} \boldsymbol{\sigma} : \dot{\mathbb{D}} : \boldsymbol{\sigma} \;&= \beta\, \dot{\zeta}\, \boldsymbol{\sigma} : \boldsymbol{G} \\ &= \beta\, \dot{\zeta}\, \boldsymbol{\sigma} : \boldsymbol{G}\, \frac{\partial_{\boldsymbol{\sigma}} \phi : \boldsymbol{\sigma}}{\partial_{\boldsymbol{\sigma}} \phi : \boldsymbol{\sigma}} \\ &= \beta\, \dot{\zeta}\, \boldsymbol{\sigma} : \frac{\boldsymbol{G} \otimes \partial_{\boldsymbol{\sigma}} \phi}{\partial_{\boldsymbol{\sigma}} \phi : \boldsymbol{\sigma}} : \boldsymbol{\sigma}. \end{aligned} \tag{20}$$

From Eq. (20), the evolution law for the 4th-order compliance tensor follows:

$$\dot{\mathbb{D}} = \beta\, \dot{\zeta}\, \frac{\boldsymbol{G} \otimes \partial_{\boldsymbol{\sigma}} \phi}{\partial_{\boldsymbol{\sigma}} \phi : \boldsymbol{\sigma}}. \tag{21}$$

The softening behavior after the onset of cracking is defined via the relation between the internal variable α and the stress-like internal variable q. According to (Meschke, Lackner, and Mang 1998) a hyperbolic function

$$q(\alpha) = f_{\mathrm{tu}} \frac{1}{(1 + \frac{\alpha}{\alpha_{\mathrm{u}}})} \tag{22}$$

is a suitable choice. α_u is a parameter which is calibrated according to the fracture energy.

4 ALGORITHMIC FORMULATION AND FINITE ELEMENT IMPLEMENTATION

This section contains details of the finite element formulation of the anisotropic elastoplastic damage model described in Subsection 3.2. Starting with the design of the enhanced strain field, the integration of the evolution equations and the linearization of the algorithm are described.

4.1 Design of the jump functions

The design of the enhanced strains is only described briefly in this subsection. Further details can be found in (Simo, Oliver, and Armero 1993) and (Mosler and Meschke 2000).

The enhanced strain field in Ω^+, or Ω^- depend on the gradient of the function $\varphi(\boldsymbol{x})$. One possible choice for the definition of $\nabla\varphi(\boldsymbol{x})$ is

$$\nabla\varphi(\boldsymbol{x}) = \sum_{i=1}^{n_{\Omega^+}} \frac{\partial N_i(\boldsymbol{\xi})}{\partial \boldsymbol{x}}, \tag{23}$$

with the standard shape functions $N_i(\boldsymbol{\xi})$. In some cases (e.g. if a crack separates one nodal point from three other points within a 4-node element), $\nabla\varphi(\boldsymbol{x})$ is not constant within a finite element. Hence, for each GAUSS point, the average value

$$\nabla\bar{\varphi} = \frac{1}{V}\int_{\Omega} \nabla\varphi(\boldsymbol{x})\, \mathrm{d}\Omega. \tag{24}$$

is taken. Using Eq. (24), the rate of the enhanced strain field can be transformed into

$$\dot{\tilde{\boldsymbol{\varepsilon}}} = \underbrace{(\nabla\bar{\varphi}\otimes\boldsymbol{m})^{\mathrm{sym}}}_{\boldsymbol{G}}\,\dot{\zeta}. \tag{25}$$

4.2 The return mapping algorithm

At the end of a time interval $[t_n,\, t_{n+1}]$, the updated state of stress and of the softening parameter q, respectively, is

$$\begin{aligned} \boldsymbol{\sigma}_{n+1} &= \mathbb{C}_{n+1} : \left(\nabla^S \bar{\boldsymbol{u}}_{n+1} - \tilde{\boldsymbol{\varepsilon}}_{n+1}\right), \\ q_{n+1} &= q_{n+1}\left(\alpha_{n+1}\right), \end{aligned} \tag{26}$$

where Eq. $(26)_a$ is defined for $\boldsymbol{x}\in\Omega^+,\Omega^-$. With the definition of a trial state

$$\boldsymbol{\sigma}^{\mathrm{tr}}_{n+1} = \mathbb{C}_n : \left(\nabla^S \bar{\boldsymbol{u}}_{n+1} - \tilde{\boldsymbol{\varepsilon}}_n\right), \tag{27}$$

Eq. (26) can be reformulated as

$$\boldsymbol{\sigma}_{n+1} = \boldsymbol{\sigma}^{\mathrm{tr}}_{n+1} - \mathbb{C}_n : \boldsymbol{G}_{n+1}\,\Delta\zeta_{n+1}. \tag{28}$$

Inserting the trial state into the failure criterion, the trial loading condition is given as

$$\phi^{\mathrm{tr}}_{n+1}(\boldsymbol{\sigma}^{\mathrm{tr}}_{n+1}, q^{\mathrm{tr}}_{n+1}) > 0 \;\text{ with: }\; q^{\mathrm{tr}}_{n+1} = q(\alpha_n). \tag{29}$$

Application of a backward EULER integration to the evolution equations (17), (10) together with the failure criterion at t_{n+1} leads to

$$\begin{aligned} \tilde{\boldsymbol{\varepsilon}}_{n+1} &= \tilde{\boldsymbol{\varepsilon}}_n + \boldsymbol{G}_{n+1}\,\Delta\zeta_{n+1}, \\ \alpha_{n+1} &= \alpha_n + \Delta\alpha_{n+1} = \alpha_n + |\Delta\zeta_{n+1}|, \\ \phi_{n+1} &= (\boldsymbol{m}_{n+1}\otimes\boldsymbol{n}_{n+1}) : \boldsymbol{\sigma}_{n+1} - q_{n+1} = 0. \end{aligned} \tag{30}$$

During the return map iteration, linearization of Eq. (26) yields (Simo and Hughes 1998),

$$\begin{aligned} \mathrm{d}\boldsymbol{\sigma}_{n+1} &= -\,\mathbb{C}_n : \mathrm{d}\tilde{\boldsymbol{\varepsilon}}_{n+1}, \\ \mathrm{d}q_{n+1} &= -\,D_{n+1}\,\mathrm{d}\alpha_{n+1}. \end{aligned} \tag{31}$$

In the k-th iteration, linearization of the residuals of Eq. (30), defined as

$$\begin{aligned} R^{\boldsymbol{\varepsilon}} &= -\tilde{\boldsymbol{\varepsilon}}_{n+1} + \tilde{\boldsymbol{\varepsilon}}_n + \boldsymbol{G}_{n+1}\,\Delta\zeta_{n+1} \\ R^{\alpha} &= -\alpha_{n+1} + \alpha_n + |\Delta\zeta_{n+1}| \end{aligned} \tag{32}$$

yields the algebraic system of equations

$$\begin{aligned} R^{\boldsymbol{\varepsilon}} + \mathrm{d}R^{\boldsymbol{\varepsilon}} &= 0, \\ R^{\alpha} + \mathrm{d}R^{\alpha} &= 0, \\ \phi_{n+1} + \mathrm{d}\phi_{n+1} &= 0. \end{aligned} \tag{33}$$

Inserting Eq. (33) into (32) leads to

$$\begin{aligned} \underbrace{\begin{bmatrix} \mathrm{d}R^{\boldsymbol{\varepsilon}} \\ \mathrm{d}R^{\alpha} \end{bmatrix}}_{\mathrm{d}\boldsymbol{R}} &= \underbrace{\begin{bmatrix} \Xi^{-1}_{n+1} & 0 \\ 0 & D^{-1} \end{bmatrix}}_{A^{-1}} \underbrace{\begin{bmatrix} \mathrm{d}\boldsymbol{\sigma}_{n+1} \\ \mathrm{d}q_{n+1} \end{bmatrix}}_{\Delta} \\ &\quad + \mathrm{d}\Delta\zeta_{n+1} \underbrace{\begin{bmatrix} \boldsymbol{G}_{n+1} \\ \mathrm{sign}\left[\mathrm{d}\Delta\zeta_{n+1}\right] \end{bmatrix}}_{\nabla M}. \end{aligned} \tag{34}$$

In Eq. (34), Ξ denotes the algorithmic moduli

$$\begin{aligned} &\Xi^{-1}_{n+1} = \mathbb{C}^{-1}_n + \mathbb{G}^{\mathrm{sym}}_{n+1} \\ &\text{with } \mathbb{G}^{\mathrm{sym}}_{n+1} = \Delta\zeta_{n+1}\left(\nabla\bar{\varphi}\otimes\frac{\partial \boldsymbol{m}_{n+1}}{\partial\boldsymbol{\sigma}_{n+1}}\right)^{\mathrm{sym}}, \\ &\text{and } [\,\mathbb{G}\,]^T_{ijkl} = [\,\mathbb{G}\,]_{jikl}. \end{aligned} \tag{35}$$

From the consistency condition

$$\mathrm{d}\phi_{n+1} = \underbrace{\begin{bmatrix} \boldsymbol{m}_{n+1}\otimes\boldsymbol{n}_{n+1} \\ -1 \end{bmatrix}}_{\nabla\phi} \underbrace{\begin{bmatrix} \mathrm{d}\boldsymbol{\sigma}_{n+1} \\ \mathrm{d}q_{n+1} \end{bmatrix}}_{\Delta}, \tag{36}$$

the change of the amplitude of the displacement jump during an iteration cycle is obtained as

$$\mathrm{d}\Delta\zeta_{n+1} = \frac{\phi_{n+1} - \nabla\phi^T\, A\, R}{\nabla\phi^T\, A\, \nabla M}. \tag{37}$$

For a globally convergent behavior at an asymptotic quadratic rate, the algorithmic tangent moduli need to

be computed from the consistent linearization of the algorithm at t_{n+1}, where the residual $\boldsymbol{R} = \boldsymbol{0}$. The algorithmic elastoplastic-damage tensor is obtained as

$$\begin{aligned} \mathbb{C}^{epd} &= \frac{\mathrm{d}\boldsymbol{\sigma}}{\mathrm{d}\nabla^S \bar{\boldsymbol{u}}} \\ &= \boldsymbol{\Xi} - \frac{\{\boldsymbol{A}\,\nabla M \otimes \nabla\phi^T\,\boldsymbol{A}\}_{[11]}}{\nabla\phi^T\,\boldsymbol{A}\,\nabla M}, \end{aligned} \tag{38}$$

where the abbreviation $\{\bullet\}_{[ij]}$ for the submatrix ij has been used. It should be noted, that the format of Eq. (38) is generally applicable to a broad range of elastoplastic as well as damage models and is not restricted to the elastoplastic damage model investigated in Subsection 3.2. Although formally identical to the algorithmic tangent operator obtained for the continuum case (Meschke, Lackner, and Mang 1998), a comparison between the tangent moduli (38) and the respective formulation for the continuum case reveals, that, although an associated flow is used, linearization results in a non symmetric 4th-order tensor $\mathbb{C}^{ep}$. Only for special cases (i.e. $\nabla f = \nabla M$), a symmetric tangent operator is recovered. It should be noted, that the proposed model affects only the material routines and not, as in most of the previous implementations of SDA-based models, the finite element level. Therefore, any computer code for nonassociated plasticity models can directly be used as the framework for the implementation of the present SDA-based elastoplastic damage model.

Based on the updated values of $\boldsymbol{\sigma}$, $\boldsymbol{m}$ and $\boldsymbol{n}$, the increment of the compliance tensor $\Delta\mathbb{D}$ is computed as

$$\Delta\mathbb{D} = \beta\,\Delta\zeta_{n+1}\,\frac{\boldsymbol{G}_{n+1} \otimes (\boldsymbol{m}_{n+1} \otimes \boldsymbol{n}_{n+1})}{(\boldsymbol{m}_{n+1} \otimes \boldsymbol{n}_{n+1}) : \boldsymbol{\sigma}_{n+1}}, \tag{39}$$

where the discrete counterpart of Eq. (21) was used.

5 NUMERICAL EXAMPLE

The applicability of the proposed finite element formulation for prognoses of mode-I fracture of brittle materials, taking stiffness degradation as well as inelastic deformations into account, is investigated by means of numerical analyses of an academic benchmark problem, an L-shaped slab (Winkler and Hofstetter 2000). The geometry and material parameters of the problem are illustrated in Fig. 3. The analysis is based on the anisotropic elastoplastic damage model described in Subsection 3.2. Since mesh independence is not the key point of this paper - this issue has been addressed, e.g. in (Oliver 1996; Mosler and Meschke 2000) - only one discretization of the slab is used in the analyses. The displacement controlled analysis is performed by means of 642 bilinear 4 node plane stress elements. Loading was applied by prescribing vertical displacements at all nodes along the right edge of the slab.

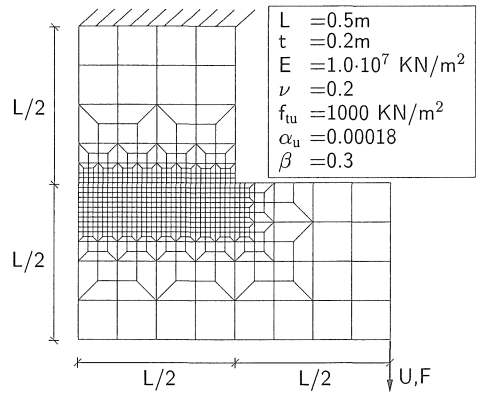

Figure 3: Geometry and material parameters used for analysis of the L-shaped slab

Fig. 4 shows the load displacement diagram obtained from the analysis. In the post-peak regime, four unloading and reloading cycles have been included. This diagram illustrates the capability of the model to capture fracture-induced stiffness degradation as well as permanent deformations after crack initiation. It should be noted, that for previously suggested implementations of damage models similar to the one used in this paper, when formulated as a rotating crack model, problems may arise in un- and reloading branches. These problems, which are connected with the mode of defining the unloading stiffness, are completely circumvented in the proposed model.

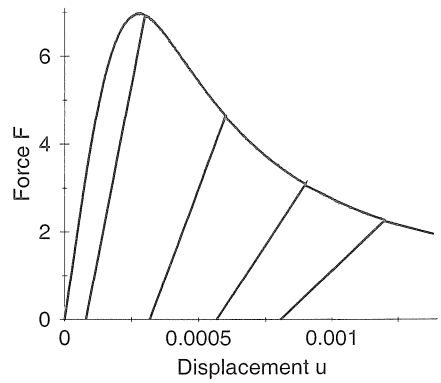

Figure 4: L-shaped slab: Load displacement diagram

Damage accumulation, characterized by the internal variable α is illustrated in Fig. 5. A localized, slightly curved crack band is observed. It refers to the final state of the loading process.

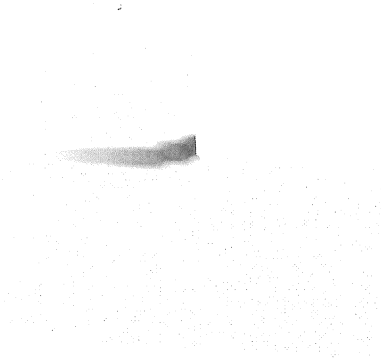

Figure 5: L-shaped slab: History variable α at the final state of deformation

6 SUMMARY AND CONCLUSIONS

The strong discontinuity approach (SDA) has been used in conjunction with an anisotropic elastoplastic-damage model for finite element analysis of mode-I fracture in quasi-brittle materials. In accordance with the corresponding continuum formulation of the model, a rotating crack approach has been used. In contrast to previous SDA-based formulations, it was shown that the amplitude of the displacement jump can be already condensed out at the material level. This leads to a considerable simplification of the implementation of this class of models within the algorithmic framework of standard plasticity models, since the necessary modifications of the FE-code are restricted to the Gauss-point level. The incorporation of the elastoplastic-damage model within the framework of the SDA is accomplished in full analogy to classical plasticity models. In contrast to previous formulations, it allows a consistent description of un- and reloading branches, taking anisotropic stiffness degradation as well as permanent deformations into account.

REFERENCES

Armero, F. (1997). Localizised anisotropic damage of brittle materials. In D. Owen, E. Oñate, and E. Hinton (Eds.), *Computational Plasticity*, Volume 1, pp. 635–640.

Jirásek, J. (2001). Embedded crack model: Part 1: Basic formulation, Part 2: Combination with smeared carcks. *International Journal for Numerical Methods in Engineering 50*, 1269–1305.

Johnson, C. and R. Scott (1981). A finite element method for problems in perfect plasticity using discontinous trial functions. In W. Wunderlich, E. Stein, and K. Bathe (Eds.), *Nonlinear finite element analysis in structual mechanics*, pp. 307–324.

Meschke, G., R. Lackner, and H. Mang (1998). An anisotropic elastoplastic-damage model for plain concrete. *International Journal for Numerical Methods in Engineering 42*, 703–727.

Mosler, J. and G. Meschke (2000). 3D FE analysis of cracks by means of the strong discontinuity approach. In E. Oñate, G. Bugeda, and B. Suárez (Eds.), *European Congress on Computational Methods in Applied Sciences and Engineering*.

Oliver, J. (1996). Modelling strong discontinuities in solid mechanics via strain softening constitutive equations Part 1: Fundamentals. Part 2: Numerical simulations. *International Journal for Numerical Methods in Engineering 39*, 3575–3623.

Simo, J. and T. Hughes (1998). *Computational inelasticity*. Springer, New York.

Simo, J., J. Oliver, and F. Armero (1993). An analysis of strong discontiniuties induced by strain softening in rate-independent inelastic solids. *Computational Mechanics 12*, 277–296.

Winkler, B. and G. Hofstetter (2000). Experimental and numerical investigations of cracking of plain and reinfored concrete. In K. Bergmeister (Ed.), *International PhD Symposium in Civil Engineering*, Volume 1, pp. 97–106.